Partial Differential Equations in Applied Mathematics 12 (2024) 100978

Contents lists available at ScienceDirect

Partial Differential Equations in Applied Mathematics

journal homepage: www.elsevier.com/locate/padiff

The modeling and mathematical analysis of the fractional-order of Cholera disease: Dynamical and Simulation

Rasha M. Yaseen [a], Nidal F. Ali [b], Ahmed A. Mohsen [c,d,*], Aziz Khan [e], Thabet Abdeljawad [e,f,g]

[a] Department of biomedical Eng., Al-Khawarzmi College of Engineering, University of Baghdad, Baghdad, Iraq
[b] Department of Medical Instrumentation Techniques Engineering, Electrical Engineering Technical College, Middle Technical University, Baghdad, Iraq
[c] Department of Mathematics, College of Education for Pure Science (Ibn Al-Haitham) University of Baghdad, Baghdad, Iraq
[d] Department of Mathematics, Open Education College, Iraq
[e] Department of Mathematics and Sciences, Prince Sultan University, P.O. Box 66833, 11586, Riyadh, Saudi Arabia
[f] Department of Mathematics and Applied Mathematics, Sefako Makgatho Health Sciences Universitu, Medusa 0204, South Africa
[g] Center for Applied Mathematics and Bioinformatics (CAMB), Gulf University for Science and Technology, 32093, Hawally, Kuwait

ARTICLE INFO

Keywords:
Cholera model
Fractional-order
Stability analysis
Sensitive analysis

ABSTRACT

In this study, a cholera model with asymptomatic carriers was examined. A Holling type-II functional response function was used to describe disease transmission. For analyzing the dynamical behavior of cholera disease, a fractional-order model was developed. First, the positivity and boundedness of the system's solutions were established. The local stability of the equilibrium points was also analyzed. Second, a Lyapunov function was used to construct the global asymptotic stability of the system for both endemic and disease-free equilibrium points. Finally, numerical simulations and sensitivity analysis were carried out using matlab software to demonstrate the accuracy and validate the obtained results.

1. Introduction

A theoretical biology has been developed by connecting mathematics and infectious diseases to discuss many phenomena and ideas. To explain such phenomena and problems, many predictions have been made. Mathematical modeling is one of the most effective methods for explaining the process and predicting its progress. Nevertheless, it remains a major challenge to define biological principles and describe them mathematically. In biological mathematics, numerous researchers have paid considerable attention to construct models of population–infectious diseases relationships. Several ideas have been introduced to interpret and predict the dynamic behavior of infectious diseases transmission especially investigating the stability of these models such as: Influenza, Covid-19, Fever, Tuberculosis and Cholera.[1–10]

Cholera is an infectious disease caused by the bacterium Vibrio Cholerae. The disease is characterized by severe diarrhea, dehydration and leg cramps, and it can be fatal if untreated. Understanding the dynamics of cholera transmission, including the role of asymptomatic carriers, is crucial for effective control and prevention. In real, the symptoms of this disease show after ingesting the water or contaminated food between (1–5) days. There are many eminent scholars have studied the cholera spread such as: Brhane et al.[11] studied the modeling of transmission cholera disease. In[12], Mukandavire et al. formulated a cholera mathematical model. Jackob et al. studied and simulated cholera model with host infection effect and vaccination.[13] Wang et al.,[14] considered the dynamics of within-host cholera disease. Al-arydah et al.[15] studied the modeling cholera disease with education and chlorination.

The fractional calculus because it can more precisely represent intricate epidemiological processes. Memory effects, non-integer time lags, and flexibility to better fit certain catchment characteristics are some of the ways it accomplishes this. As a result, modeling accuracy is increased, particularly when it comes to simulating the long-term behaviors and scaling characteristics of epidemiological systems. As well as, the fractional derivative improve our model by taking into account the memory effect. Because it is a nonlocal operator, while the classical ordinary derivative is a local operator which is unable to model the hereditary properties and memory effect. Also, when cholera infection spreads within a population, individuals acquire knowledge about this disease. For more details, for the use and application of fractional derivative in biology we have added the following references: Hattaf and Mohsen studied the dynamics of a generalized fractional modeling of corona virus with carrier effect[16]. Also, Gacem et al.,[17] proposed a fractional mathematical model of SEIR epidemic model with time delay. In[18], Ahmad et al. studied a fractional smoking epidemic

* Corresponding author at: Department of Mathematics, College of Education for Pure Science (Ibn Al-Haitham) University of Baghdad, Baghdad, Iraq.
E-mail addresses: aamuhseen@gmail.com (A.A. Mohsen), akhan@psu.edu.sa (A. Khan).

https://doi.org/10.1016/j.padiff.2024.100978
Received 8 September 2024; Received in revised form 25 October 2024; Accepted 2 November 2024
Available online 12 November 2024

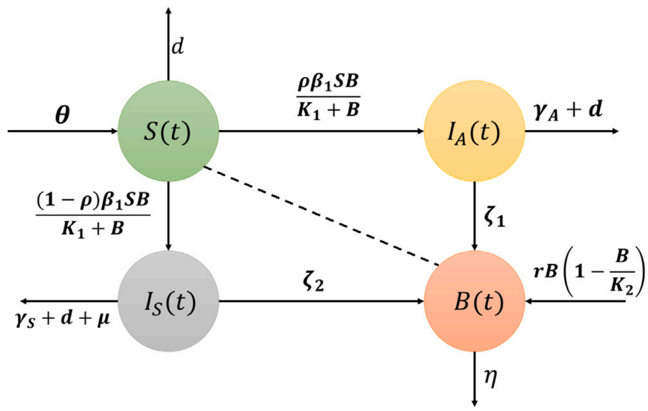

Fig. 1. Diagram of cholera model.

model. Also, other researchers have recently presented the modeling of cholera disease using fractional-order derivative see[19–29]. The rest of this paper is organized as follows. In Section 2, we present the cholera model with a fractional-order effect. In Section 3, we analyze the model by considering the boundedness, positivity and equilibrium points as well as calculated the basic reproduction number. The local and global stability of equilibrium points in Sections 4 and 5. In Section 6, numerical simulations are carried out to enhance our comprehension of the system's dynamics. Additionally, a sensitivity analysis is conducted to identify the crucial parameters of the system. Lastly, in Section 7, we summarize the findings of this study as our conclusion.

2. Model formulation

The Cholera disease has caused a great deal of stress on the world health system, leading to a high death toll. Some authors have utilized mathematical models to study and analyze the outbreak of Cholera disease. The authors in[30] was proposed the classical Cholera model is formulated by the following order differential equations system and the diagram (Fig. 1):

$$\begin{aligned}
\frac{dS}{dt} &= \theta - \frac{\beta_1 SB}{K_1+B} - dS,\\
\frac{dI_A}{dt} &= \frac{\rho\beta_1 SB}{K_1+B} - (\gamma_A + d)I_A,\\
\frac{dI_S}{dt} &= \frac{(1-\rho)\beta_1 SB}{K_1+B} - (\gamma_S + d + \mu)I_S,\\
\frac{dR}{dt} &= \gamma_A I_A + \gamma_S I_S - dR,\\
\frac{dB}{dt} &= rB(1 - \frac{B}{K_2}) - \eta B + \zeta_1 I_A + \zeta_2 I_S.
\end{aligned} \tag{2.1}$$

Thus, in order to include the memory impact and the past history to get a better understanding of the dynamics of Cholera disease under Holling Type II functional response, we reformulate the model (2.1) by using the Caputo fractional derivative as follows:

$$\begin{aligned}
D^\alpha S(t) &= \theta - \frac{\beta_1 SB}{K_1+B} - dS; \quad S(0) > 0,\\
D^\alpha I_A(t) &= \frac{\rho\beta_1 SB}{K_1+B} - (\gamma_A + d)I_A; \quad I_A(0) \geq 0,\\
D^\alpha I_S(t) &= \frac{(1-\rho)\beta_1 SB}{K_1+B} - (\gamma_S + d + \mu)I_S; \quad I_S(0) \geq 0,\\
D^\alpha R(t) &= \gamma_A I_A + \gamma_S I_S - dR; \quad R(0) \geq 0,\\
D^\alpha B(t) &= rB(1 - \frac{B}{K_2}) - \eta B + \zeta_1 I_A + \zeta_2 I_S; \quad B(0) \geq 0.
\end{aligned} \tag{2.2}$$

Here, D^α denotes the Caputo derivative for $0 < \alpha \leq 1$. While, $S(t)$, $I_A(t)$, $I_S(t)$, $R(t)$ and $B(t)$ represent the densities at time t for the susceptible humans, asymptomatic infectious humans, symptomatic infectious humans, recovered humans and bacterial source of disease respectively. It is assumed that males and females grows logistically. Accordingly, the parameters can be described as in Table 1.

Table 1
Definitions of model parameters.

Parameter	Biological Meaning
θ	The birth rate,
β_1	The contact rate,
$\rho \in [0,1]$	The fraction rate,
$K_i, i = 1,2$	The carrying capacity,
d	The death rate,
μ	The death rate due to disease from I_S,
γ_A, γ_S	The recovery rates,
r	The intrinsic growth rate,
η	The decay rate of B,
$\zeta_i, i = 1,2$	Represents an increase in sources of infection,
$S(0)$, $I_A(0)$, $I_S(0)$, $R(0)$ and $B(0)$	The initial points

3. Fundamental mathematical results and equilibrium points

In this section, the basic mathematical properties of the model are explored. This consists of the positivity and boundedness of the solution of model (2.2). Also, the computation of equilibrium points and basic reproduction number. We assert that in the following subsections:

3.1. Positivity and boundedness

Now in this subsection, we show that, the model have a positive solutions. First, we assume that the all parameters of fractional model are positive, we get the following:

$$\begin{aligned}
&D^\alpha S(t)|_{S=0} = \theta > 0,\\
&D^\alpha I_A(t)|_{I_A=0} = \frac{\rho\beta_1 SB}{K_1+B} > 0, \forall\ S > 0, B > 0,\\
&D^\alpha I_S(t)|_{I_S=0} = \frac{(1-\rho)\beta_1 SB}{K_1+B} > 0, \forall\ S > 0,\ B > 0,\\
&D^\alpha R(t)|_{R=0} = \gamma_A I_A + \gamma_S I_S > 0, \forall\ I_A > 0, I_S > 0,\\
&D^\alpha B(t)|_{B=0} = \zeta_1 I_A + \zeta_2 I_S > 0, \forall\ I_A > 0,\ I_S > 0.
\end{aligned} \tag{3.1}$$

As a result, we can observe that the solution of model (2.2) is non-negative.

Theorem 1. *Every solutions of model (2.2) are bounded.*

Proof. Let $N(t) = S(t) + I_A(t) + I_S(t) + R(t)$, then

$D^\alpha N(t) \leq \theta - dN(t)$.

Therefore,

$D^\alpha N(t) + dN(t) \leq \theta$.

Taking the Laplace transform on both sided yields

$$\mathcal{L}(D^\alpha N(t)) = \frac{\theta}{\lambda} - d\mathcal{L}(N(t)).$$

Simplifying this equation, we have the following inequality

$$\mathcal{L}(N(t)) \leq \frac{\theta\lambda^{-1}}{\lambda^\alpha + d} + \frac{\lambda^{\alpha-1}N(0)}{\lambda^\alpha + d}.$$

Now, taking the inverse Laplace transform and using the fact that

$$\mathcal{L}^{-1}\left[\frac{\lambda^{-(\alpha-\beta)}}{\lambda^\beta - \alpha}\right] = t^{\alpha-1}E_{\beta,\alpha}(\alpha t^\beta), \alpha, \beta > 0, \lambda^\alpha > |\alpha|,$$

where, $E_{\alpha,\beta(.)}$ is the Mittag-Leffler function defined in[31], we have

$$\begin{aligned}
N(t) &\leq \theta t^\alpha E^{\alpha,\alpha+1}(-dt^\alpha) + N(0)E_{\alpha,1}(-dt^\alpha)\\
&= \theta t^\alpha E^{\alpha,\alpha+1}(-dt^\alpha) + N(0)\left[-dt^\alpha E_{\alpha,\alpha+1}(-dt^\alpha) + \frac{1}{\Gamma(1)}\right]\\
&\leq \theta t^\alpha E^{\alpha,\alpha+1}(-dt^\alpha) + \frac{\theta}{d}\left[-dt^\alpha E_{\alpha,\alpha+1}(-dt^\alpha) + \frac{1}{\Gamma(1)}\right]\\
&= \frac{\theta}{d\Gamma(1)} = \frac{\theta}{d}.
\end{aligned} \tag{3.2}$$

Then, for any $X(0)$, we have $N(t) \leq \frac{\theta}{d}$. Hence the feasible and bounded region for model (2.2) initiate in $\mathcal{R}^5_+$ and

$$\Gamma = \left\{ S(t), I_A(t), I_S(t), R(t) \in \mathcal{R}^4 : 0 \le N(t) \le \frac{\theta}{d},\ 0 \le B \le \frac{rK_2}{4} \right\}.$$

3.2. Equilibrium points

In this subsection, since the variable $R(t)$ does not appear in other equations of model (2.2), we can reduce this model and rewrite it without 4th equation. Now, the fixed points are obtained from the equilibrium state condition $D^\alpha S(t) = 0$, $D^\alpha I_A(t) = 0$, $D^\alpha I_S(t) = 0$ and $D^\alpha B(t) = 0$. i.e.,

$$\begin{aligned} &\theta - \tfrac{\beta_1 SB}{K_1+B} - dS = 0,\\ &\tfrac{\rho\beta_1 SB}{K_1+B} - (\gamma_A + d)I_A = 0,\\ &\tfrac{(1-\rho)\beta_1 SB}{K_1+B} - (\gamma_S + d + \mu)I_S = 0,\\ &rB(1 - \tfrac{B}{K_2}) - \eta B + \zeta_1 I_A + \zeta_2 I_S = 0. \end{aligned} \tag{3.3}$$

Biologically, model (3.3) have two equilibrium points, namely:

- The infected free equilibrium point (IFEP), $E_1 = \left(\frac{\theta}{d}, 0, 0, 0\right)$.

Then, by the results of the method of the next generation matrix, one obtains the basic reproduction number of system (3.3) as follows and denoted by $\mathbb{R}_0$:

$$\mathbb{R}_0 = Max.\left\{ \left(\frac{r\theta\beta_1\rho\zeta_1}{(d\eta^3 K_1)(\gamma_A + d)} \right), \left(\frac{(1-\rho)r\theta\beta_1\zeta_2}{(d\eta^3 K_1)(\gamma_S + d + \mu)} \right) \right\}. \tag{3.4}$$

- The endemic equilibrium point (EEP), $E_2 = \left(S_2, I_{A2}, I_{S2}, B_2\right)$,

where

$$S_2 = \frac{\theta(K_1 + B_2)}{G},\quad I_{A2} = \frac{\rho\theta\beta_1 B_2}{G(\gamma_A + d)},\quad I_{S2} = \frac{(1-\rho)\theta\beta_1 B_2}{G(\gamma_S + d + \mu)},$$

Here, $G = \beta_1 B_2 + d(K_1 + B_2)$ while B_2 is a positive root of the following 4th order equation:

$$A_1 B_2^4 + A_2 B_2^3 + A_3 B_2^2 + A_4 B_2 = 0. \tag{3.5}$$

Where,

$$\begin{aligned} A_1 &= -r(\beta_1 + d)(\gamma_A + d)(\gamma_S + d + \mu) < 0,\\ A_2 &= (\gamma_A + d)(\gamma_S + d + \mu)\left[rK_2(\beta_1 + d) - (rK_1(\beta_1 + 2d) + \eta K_2(\beta_1 + d))\right],\\ A_3 &= \theta\beta_1 K_2\left[\rho\zeta_1(\gamma_S + d + \mu) + \zeta_2(1-\rho)(\gamma_A + d)\right]\\ &\quad + rK_1K_2(\beta_1 + 2d)(\gamma_A + d)(\gamma_S + d + \mu)\\ &\quad - \left[\eta K_1K_2(\beta_1 + 2d)(\gamma_A + d)(\gamma_S + d + \mu) + rdK_1^2(\gamma_A + \gamma_S + 2d + \mu)\right],\\ A_4 &= K_1K_2\left[rd + (\gamma_A + d)\left(\theta\beta_1\zeta_2(1-\rho) - d\eta K_1\right) + (\gamma_S + d + \mu)\left(\mathbb{R}_0 - 1\right)\right]. \end{aligned}$$

Now, Eq. (3.5) has a unique positive root and the endemic equilibrium point (EEP) exists when $\mathbb{R}_0 > 1$, that guarantees $A_4 > 0$ with one of the conditions $A_3 > 0$ or $A_2 < 0$ is holds.

In the next section, the local stability conditions of $IFEP$ and EEP is performed. Both equilibrium points are discussed according to $\mathbb{R}_0$ and using the Routh–Hurwitz criteria.

4. Local stability analysis

Theorem 2. *If $\mathbb{R}_0 < 1$ and the following condition (4.1) is holds, then the infected-free equilibrium point (IFEP) is strictly locally asymptotically stable.*

$$r < \eta. \tag{4.1}$$

Proof. The Jacobian matrix associated at $(IFEP)$ of model (3.3) is given by:

$$J(E_1) = \begin{pmatrix} -d & 0 & 0 & \frac{-\theta\beta_1}{dK_1}\\ 0 & -(\gamma_A + d) & 0 & \frac{\rho\theta\beta_1}{dK_1}\\ 0 & 0 & -(\gamma_S + d + \mu) & \frac{(1-\rho)\theta\beta_1}{dK_1}\\ 0 & \zeta_1 & \zeta_2 & r - \eta \end{pmatrix}, \tag{4.2}$$

with the characteristic equation

$$(\lambda + d)\left[\lambda^3 + C_1\lambda^2 + C_2\lambda + C_3\right] = 0. \tag{4.3}$$

Where

$$\begin{aligned} C_1 &= -\left(r - \eta - (\gamma_A + d) - (\gamma_S + d + \mu)\right),\\ C_2 &= -(\gamma_A + d)\left(r - \eta - (\gamma_S + d + \mu)\right) - (r - \eta)(\gamma_S + d + \mu) - \tfrac{\rho\theta\beta_1\zeta_1}{dK_1}\\ &\quad - \tfrac{(1-\rho)\theta\beta_1\zeta_2}{dK_1},\\ C_3 &= \tfrac{\theta\beta_1\zeta_2(1-\rho)(\gamma_A + d)}{dK_1} - (\gamma_S + d + \mu)\left(\mathbb{R}_0 - 1\right),\\ C_1C_2 - C_3 &= -(r - \eta)\left((\gamma_A + d)^2 - (r - \eta)(\gamma_S + d + \mu)\right)\\ &\quad + \left(r - \eta - (\gamma_S + d + \mu)\right)\left(\mathbb{R}_0 - 1\right)\\ &\quad + \left((r - \eta)(\gamma_A + d)\right)\left(\mathbb{R}_0 - 1 - (\gamma_S + d + \mu)^2\right). \end{aligned}$$

Since the first eigenvalue of Eq. (4.3) is $\lambda_1 = -d$, and it is strictly negative. Thus, the remaining other eigenvalues $\lambda_i, i = 2, 3, 4$ are solution of Eq. (4.3).

Clearly, if the condition (4.1) is hold with $\mathbb{R}_0 < 1$, and according to the Routh–Hurwitz criteria are necessary and sufficient for the Matignon criterion $C_i > 0, i = 1, 3, C_1C_2 - C_3 > 0$ and $\left|arg(\lambda_i)\right| > \alpha\pi/2$ $\forall\alpha \in (0, 1], i = 1, 2, 3, 4$. Therefore, all eigenvalues have negative real parts, we conclude that the infected-free equilibrium point (IFEP) of the model (3.3) is locally asymptotically stable under condition (4.1).

Theorem 3. *If $\mathbb{R}_0 > 1$ and the following conditions (4.4) are hold, then the endemic equilibrium point (EEP) is strictly locally asymptotically stable.*

$$\begin{aligned} &d > Max.\left\{\zeta_1 - \gamma_A,\ \zeta_2 - (\gamma_S + \mu)\right\},\\ &\eta K_2 + 2rB_2 > rK_2. \end{aligned} \tag{4.4}$$

Proof. The Jacobian matrix associated at (EEP) of model (3.3) is given by:

$$J(E_2) = \begin{pmatrix} q_{11} & 0 & 0 & q_{14}\\ q_{21} & q_{22} & 0 & q_{24}\\ q_{31} & 0 & q_{33} & q_{34}\\ 0 & q_{42} & q_{43} & q_{44} \end{pmatrix}, \tag{4.5}$$

where

$q_{11} = -\left(\frac{\beta_1 B_2}{K_1+B_2} + d\right)$; $q_{14} = \frac{-\beta_1 K_1 S_2}{(K_1+B_2)^2}$; $q_{21} = \frac{\rho\beta_1 B_2}{K_1+B_2}$; $q_{22} = -(\lambda_A + d)$; $q_{24} = \frac{\rho\beta_1 K_1 S_2}{(K_1+B_2)^2}$; $q_{31} = \frac{(1-\rho)\beta_1 B_2}{K_1+B_2}$; $q_{33} = -(\lambda_S + d + \mu)$; $q_{34} = \frac{(1-\rho)\beta_1 K_1 S_2}{(K_1+B_2)^2}$; $q_{42} = \zeta_1$; $q_{43} = \zeta_2$; $q_{44} = r - \eta - \frac{2rB_2}{K_2}$.

By applying Gershgorin's first theorem,[32] we obtain that the all eigenvalues of (4.5) have the negative real part when $\left|q_{ii}\right| > \sum_{i=1;\ i\ne j}^{4} \left|q_{ij}\right|$. Due to the high dimensionality of the system, and the highly non-trivial Jacobian, an local stability analytical proof seems hardly achievable. So, We conjecture that this is true of $\mathbb{R}_0 > 1$ and conditions (4.4). Thus, the numerical exploration of the model seems to confirm this result. we conclude that the endemic equilibrium point (EEP) of the model (3.1) is locally asymptotically stable.

5. Global stability analysis

Theorem 4. *The model (3.3) at the infection-free equilibrium point (IFEP) is GAS if $\mathbb{R}_0 < 1$ with the conditions (4.1) and (5.1)*

$$8d\beta_1 < r < 1. \tag{5.1}$$

Proof. Let us define the positive function V_1 as follows

$$V_1(t) = (S_1(t) - S(t)) + I_A(t) + I_S(t) + B(t). \tag{5.2}$$

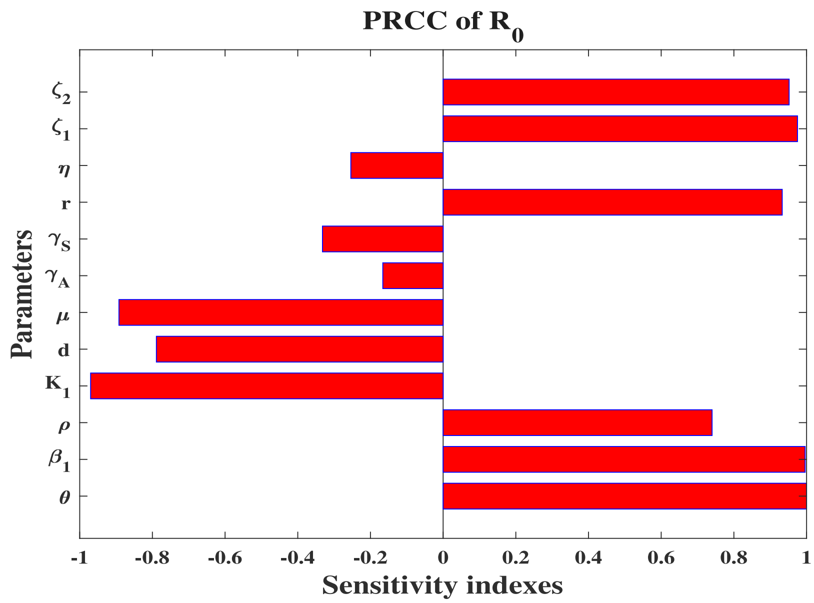

Fig. 2. Sensitivity analysis of the model according to the parameters related to $\mathbb{R}_0$.

The fractional derivative of order α in the sense of Caputo of V_1 can be expressed as

$$D^{\alpha}V_1(t) = -D^{\alpha}S(t) + D^{\alpha}I_A(t) + D^{\alpha}I_S(t) + D^{\alpha}B(t). \tag{5.3}$$

$$D^{\alpha}V_1(t) = -\theta + \frac{\beta_1 SB}{K_1+B} + dS + \theta - dS_1 + \frac{\rho\beta_1 SB}{K_1+B} - \gamma_A I_A - dI_A + \frac{(1-\rho)\beta_1 SB}{K_1+B}$$
$$-\gamma_S I_S - dI_S - \mu I_S + rB(1-\frac{B}{K_2}) - \eta B + \zeta_1 I_A + \zeta_2 I_S.$$

By utilizing the results in[31] we get

$$D^{\alpha}V_1(t) = d\left(S - \frac{\theta}{d}\right) - (\gamma_A + d - \zeta_1)I_A - (\gamma_S + d + \mu - \zeta_2)I_S$$
$$+ B\left[(r-\eta) - \frac{rB}{K_2} + \frac{2\beta_1\theta}{d(K_1+B)}\right].$$

For $\mathbb{R}_0 < 1$ then $\gamma_A + d - \zeta_1 > 0$ and $\gamma_S + d + \mu - \zeta_2 > 0$. Thus, $D^{\alpha}V_1(t) \le 0$ when the condition (5.1) is holds. Thus by LaSalle's invariance principle, we conclude that the infection-free equilibrium point (IFEP) is globally asymptotically stable.

Theorem 5. *The model (3.3) at the endemic equilibrium point (EEP) is GAS if $\mathbb{R}_0 > 1$ and under the following conditions*

$$\begin{aligned} &U_{12}^2 < \tfrac{2}{3}U_{11}U_{22},\\ &U_{13}^2 < \tfrac{2}{3}U_{11}U_{33},\\ &U_{14}^2 < \tfrac{4}{9}U_{11}U_{44},\\ &U_{24}^2 < \tfrac{2}{3}U_{22}U_{44},\\ &U_{34}^2 < \tfrac{2}{3}U_{33}U_{44}, \end{aligned} \tag{5.4}$$

We will mention all the symbols in the proof.

Proof. Let us define the positive function V_1 as follows

$$V_2(t) = \frac{(S-S_2)^2}{2} + \frac{(I_A - I_{A1})^2}{2} + \frac{(I_S - I_{S1})^2}{2} + \frac{(B-B_2)^2}{2}. \tag{5.5}$$

The fractional derivative of order α in the sense of Caputo of V_2 can be expressed as

$$D^{\alpha}V_2(t) = (S-S_1)D^{\alpha}S(t) + (I_A - I_{A1})D^{\alpha}I_A(t) + (I_S - I_{S1})D^{\alpha}I_S(t) + (B-B_1)D^{\alpha}B(t). \tag{5.6}$$

Therefore, by simplify Eq. (5.6) according to model (3.3) we get

$$\begin{aligned} D^{\alpha}V_2(t) = &-\left[\tfrac{U_{11}}{3}(S-S_1)^2 - U_{12}(S-S_1)(I_A-I_{A1}) + \tfrac{U_{22}}{2}(I_A-I_{A1})^2\right]\\ &-\left[\tfrac{U_{11}}{3}(S-S_1)^2 - U_{13}(S-S_1)(I_S-I_{S1}) + \tfrac{U_{33}}{2}(I_S-I_{S1})^2\right]\\ &-\left[\tfrac{U_{11}}{3}(S-S_1)^2 - U_{14}(S-S_1)(B-B_1) + \tfrac{U_{44}}{3}(B-B_1)^2\right]\\ &-\left[\tfrac{U_{22}}{2}(I_A-I_{A1})^2 - U_{24}(I_A-I_{A1})(B-B_1) + \tfrac{U_{44}}{3}(B-B_1)^2\right]\\ &-\left[\tfrac{U_{33}}{2}(I_S-I_{S1})^2 - U_{34}(I_S-I_{S1})(B-B_1) + \tfrac{U_{44}}{3}(B-B_1)^2\right]. \end{aligned}$$

By utilizing the conditions (5.4) we have

$$\begin{aligned} D^{\alpha}V_2(t) \le &-\left[\sqrt{\tfrac{U_{11}}{3}}(S-S_1) - \sqrt{\tfrac{U_{22}}{2}}(I_A-I_{A1})\right]^2\\ &-\left[\sqrt{\tfrac{U_{11}}{3}}(S-S_1) - \sqrt{\tfrac{U_{33}}{2}}(I_S-I_{S1})\right]^2\\ &-\left[\sqrt{\tfrac{U_{11}}{3}}(S-S_1) - \sqrt{\tfrac{U_{44}}{3}}(B-B_1)\right]^2\\ &-\left[\sqrt{\tfrac{U_{22}}{2}}(I_A-I_{A1}) - \sqrt{\tfrac{U_{44}}{3}}(B-B_1)\right]^2\\ &-\left[\sqrt{\tfrac{U_{33}}{2}}(I_S-I_{S1}) - \sqrt{\tfrac{U_{44}}{3}}(B-B_1)\right]^2 \end{aligned}$$

Where

$$U_{11} = d + \frac{\beta_1 B_1(B+K_1)}{Z_1} \;;\; U_{22} = \gamma_A + d \;;\; U_{12} = \frac{\rho\beta_1 B_1(B+K_1)}{Z_1};$$
$$U_{13} = \frac{(1-\rho)\beta_1 B_1(B+K_1)}{Z_1} \;;\; U_{14} = \frac{\beta_1 K_1 S}{Z_1} \;;\; U_{33} = \gamma_S + d + \mu$$
$$U_{34} = \frac{(1-\rho)\beta_1 K_1 S_1}{Z_1} + \zeta_2 \;;\; U_{44} = \eta - r + \frac{r(B+B_1)}{K_2} \;;\; U_{24} = \frac{\rho\beta_1 K_1}{Z_1} + \zeta_1.$$

Observe that $D^{\alpha}V_2(t) = 0$ at $E_2 = \left(S_2, I_{A2}, I_{S2}, B_2\right)$, and $D^{\alpha}V_2(t) \le 0$ if $\mathbb{R}_0 > 1$ and the conditions (5.4) are satisfied. Hence, we concluded that the endemic equilibrium point E_2 is globally asymptotically stable.

6. Numerical simulation

6.1. Sensitivity analysis

To study the impact of parameters on the model (3.3), we perform a sensitivity analysis in this subsection. Sensitivity indices indicate whether the parameters have a positive or negative impact on the

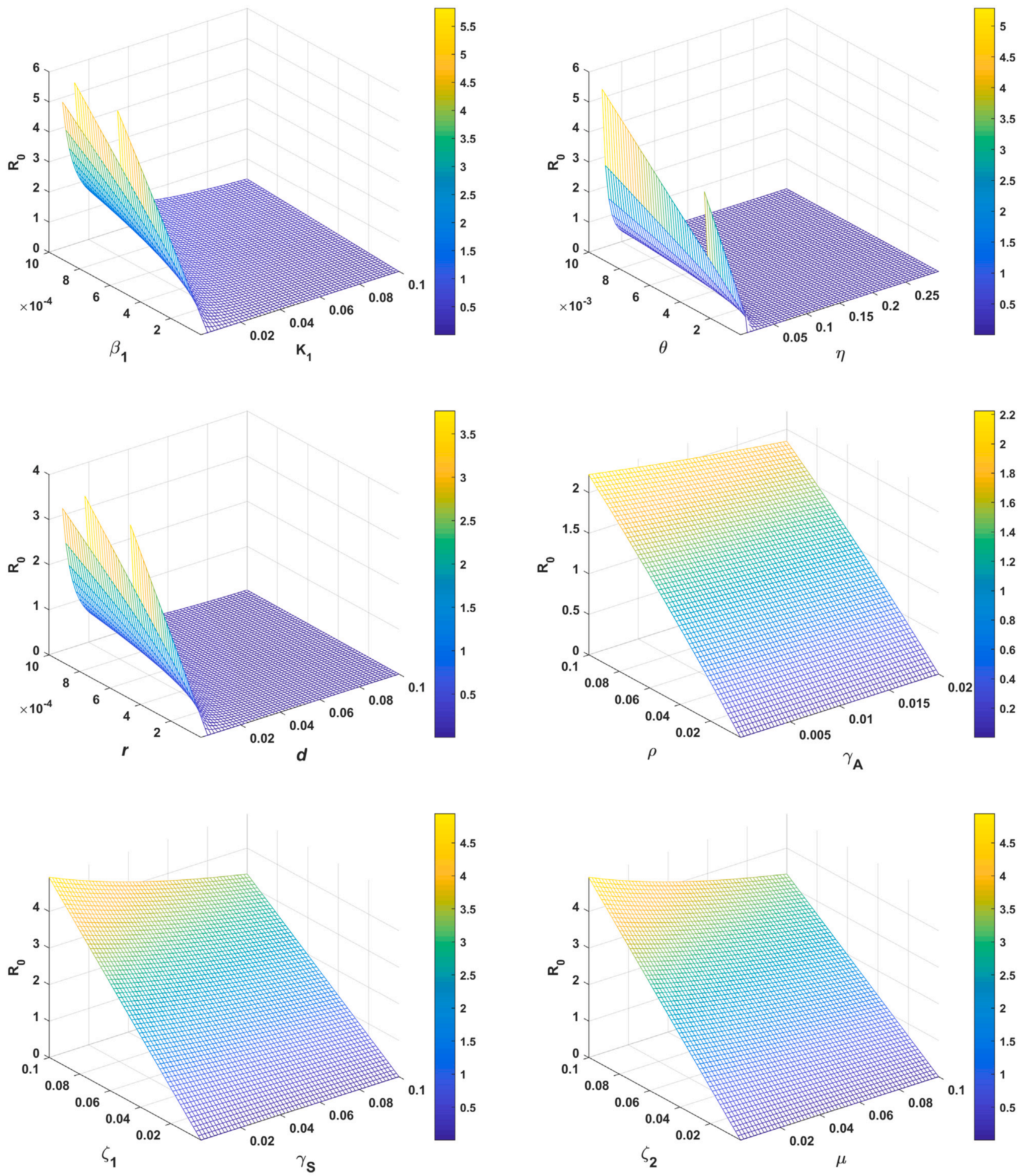

Fig. 3. Results graphs of $\mathbb{R}_0$ according to the parameters of model (3.3).

model (3.3). We have discussed the sensitivity indices of the parameters on $\mathbb{R}_0$, to more info see[33], Using methodology or approach, we quantified the influence of each parameter. The results show that describe main findings, e.g., certain parameters significantly increase or decrease the basic reproduction number, highlighting their critical role in the system's behavior. Then, we put the parameters values as

$$\begin{aligned} &\theta = 20\ ;\ \beta_1 = 0.01\ ;\ K_1 = 0.1\ ;\ d = 0.1\ ;\ \rho = 0.2\ ;\ \gamma_A = 0.02\ ;\ \gamma_S = 0.1; \\ &\mu = 0.1\ ;\ r = 0.1\ ;\ K_2 = 80\ ;\ \eta = 0.3\ ;\ \zeta_1 = 0.1\ ;\ \zeta_2 = 0.1. \end{aligned} \tag{6.1}$$

Definition 1. The normalized forward sensitivity index of a variable W is denoted by $\mathbb{R}_0$, and it is defined as:

$$\Pi_W^{\mathbb{R}_0} = \frac{\partial \mathbb{R}_0}{\partial W} \cdot \frac{W}{\mathbb{R}_0}.$$

The results of the sensitivity analysis indicate that the model parameters with a positive sensitivity index increase the value of $\mathbb{R}_0$ as they increase, meaning the disease will spread. Conversely, those with a negative sensitivity index decrease the value of $\mathbb{R}_0$ as they

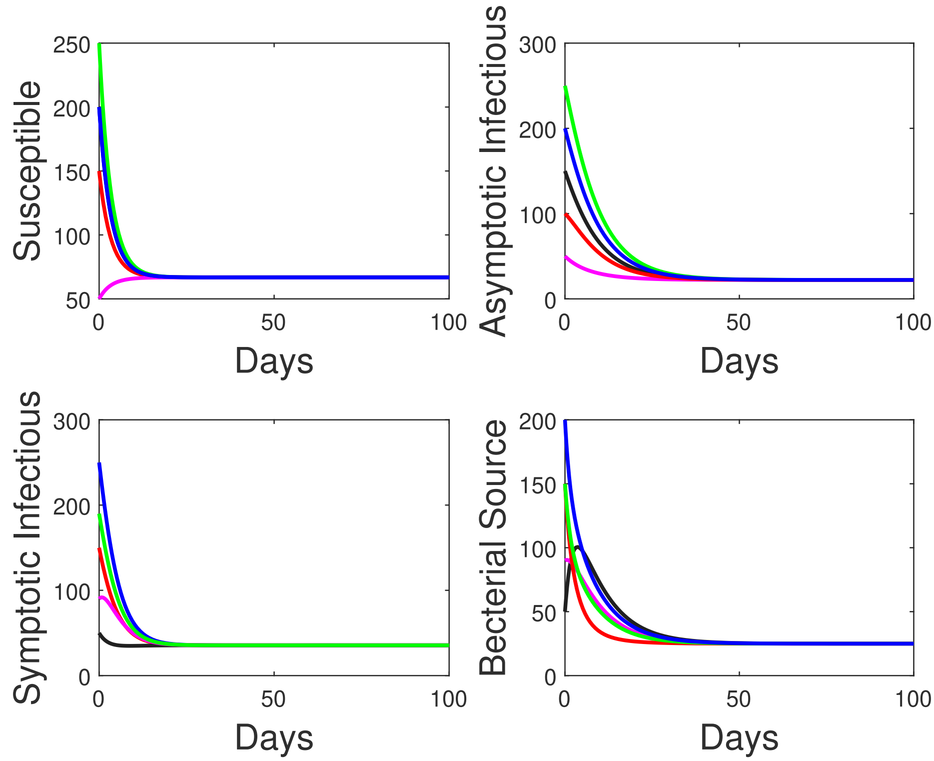

Fig. 4. Model dynamics illustrating the global stability of the E_2.

Table 2
Sensitivity values of the parameters associated to $\mathbb{R}_0$.

Parameter	Sensitivity indices
θ	1
β_1	0.996
ρ	0.74
K_1	−0.97
d	−0.789
μ	−0.892
γ_A	−0.166
γ_S	−0.332
r	0.993,
η	−0.254
ζ_1	0.975
ζ_2	0.952

increase, indicating that the disease will fade away. Therefore, the normalized sensitivity index value for each parameter used in model (3.3) is summarized in Table 2 with shows the results in the Figs. 2 and 3.

Clearly, Fig. 3, it is clear that the system parameters have varying effects on $\mathbb{R}_0$, increasing the value of certain parameters has a positive impact on $\mathbb{R}_0$, such as, θ, β_1, r, ρ, ζ_1, ζ_2. While increasing the value of other parameters has a negative impact for example K_1, d, η, μ, γ_A, γ_S.

6.2. Numerical analysis

In this subsection, we analyze the fractional-order derivative cholera model (3.3) using the parameters specified in Eq. (6.1). We illustrate the model's equations graphically to study the disease dynamics. The dynamics of the globally asymptotically stable endemic equilibrium point E_2 from various initial conditions are depicted in Fig. 4.

Obviously, Fig. 4 shows the ownership of model (3.3) using Dataset (6.1) with a unique EE that is GAS. In the following we shows to the influence of infection rate β on the dynamics of model (3.3) is shown in Fig. 5.

Now, setting the infection rate value $\beta = 0.0001$, and keeping the other parameter values from Eq. (6.1), we find that the trajectory of model (3.3) approaches the infection-free equilibrium point E_1, as shown in Fig. 5.

According Fig. 5, decreasing the value of infection rate beta reduces the stability of E_2, and the model approaches to E_1.

The numerical results of the model Eqs. (3.3) in response to the fractional order memory index α are presented in Figs. 6 and 7. The cholera model dynamics are described based on the choice of different memory indices.

7. Conclusion and results

Mathematical modeling of cholera disease using fractional-order differential equations with of both asymptomatic and symptomatic compartments provides a comprehensive understanding of the disease dynamics. This approach allows for capturing the complexities and memory effects in disease transmission, leading to better-informed public health strategies and interventions. First, we have studied the boundedness, positivity and equilibrium points as well as expression of the epidemic threshold by $\mathbb{R}_0$ is derived of the proposed model. The theoretical results implies that the system has a stable to infected-free equilibrium point $(IFEP)$ when $\mathbb{R}_0 < 1$ with condition (4.1) and a unique endemic equilibrium point (EEP) when $\mathbb{R}_0 > 1$ with conditions (4.4). The (GAS) of each equilibrium points are established using Lyapunov function. It is observed that the fractional order of the derivative and basic reproduction number play a crucial role in the stability behavior of the equilibrium points.

The numerical results show that the dynamical trajectories approaches to the equilibrium points as fast as the fractional order ($\alpha \longrightarrow 1$). Therefore, we can understand that the stability of the equilibrium

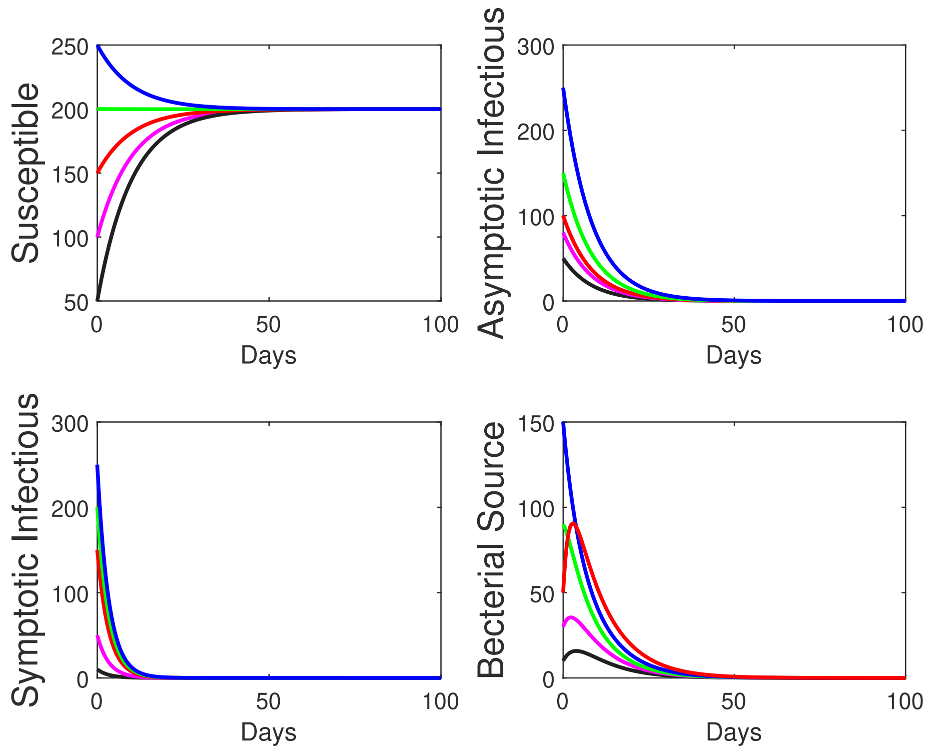

Fig. 5. Model dynamics illustrating the global stability of the E_1.

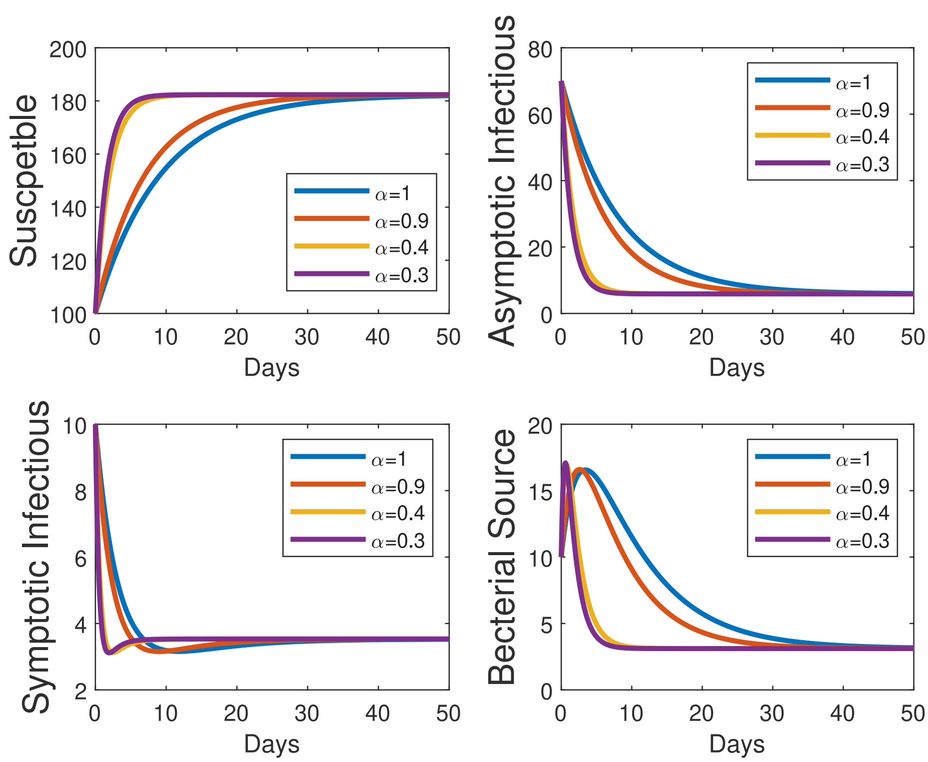

Fig. 6. Impact of fractional memory index α on population at E_2.

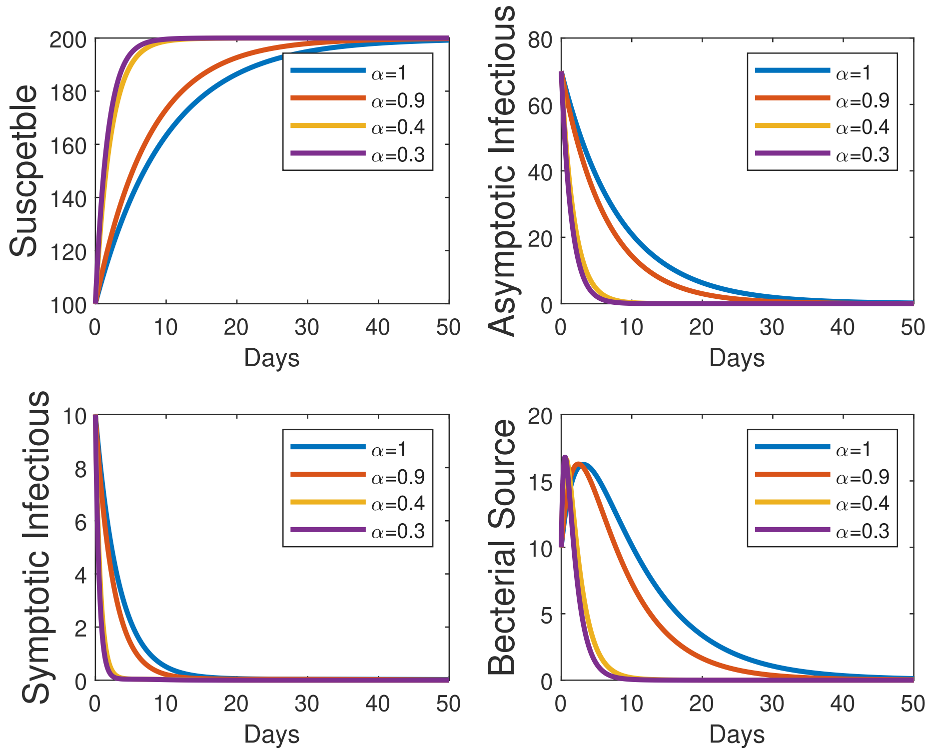

Fig. 7. Impact of fractional memory index α on population at E_1.

points is independent of different fractional-order derivatives, while the fractional-order derivative only affects the time to reach the stationary states. Also, the simulation works of the control problem suggest that in the presence of memory, optimal application of treatment control reduces the number of infected individual (See Figs. 6 and 7). Moreover, from sensitivity analysis it is found that the birth, contact, intrinsic growth rates and the increase in sources of infection rate of cholera have the negative effect on $\mathbb{R}_0$. But, the other parameters as death, recovery and the decay rates have the positive effect on $\mathbb{R}_0$ (See Figs. 2 and 3).

Declaration of competing interest

The authors declare that they have no known competing financial interests or personal relationships that could have appeared to influence the work reported in this paper.

Data availability

No data was used for the research described in the article.

References

1. Yaseen RM, Mohsen AA, Al-Husseiny HF, Hattaf k. Stability and hopf bifurcation of an epidemiological model with effect of delay the awareness programs and vaccination: analysis and simulation. *Commun Math Biol Neurosci.* 2023;2023:32.
2. AL-Husseiny HF, Ali NF, Mohsen AA. The effect of epidemic disease outbreaks on the dynamic behavior of a prey-predator model with Holling type II functional response. *Commun Math Biol Neurosci.* 2021;2021:72.
3. Mohsen AA, AL-Husseiny HF, Naji RK. The dynamics of Coronavirus pandemic disease model in the existence of a curfew strategy. *J Interdiscip Math.* 2022;25(6):1777–1797. http://dx.doi.org/10.1080/09720502.2021.2001139.
4. Oshinubi K, Peter O, Addai E, et al Mathematical modelling of tuberculosis outbreak in an East African country incorporating vaccination and treatment. *Computation.* 2023;11(7):143. http://dx.doi.org/10.3390/computation11070143.
5. Al-arydah M, Madhu K. Optimal vaccine for human papillomavirus and age-difference between partners. *Math Comput Simulation.* 2021;185:325–346.
6. Chavez CC, Song B. Dynamical models of tuberculosis and their applications. *Math Biosci Eng.* 2004;1(2):361–404.
7. Aguiar M, Stollenwerk N. Mathematical models of dengue fever epidemiology: multi-strain dynamics, immunological aspects associated to disease severity and vaccines. *Commun Bio-math Sci.* 2017;1(1):1–12.
8. Bowong S, Tewa JJ. Mathematical analysis of a tuberculosis model with differential infectivity. *Commun Nonlinear Sci.* 2009;14:4010–4021. http://dx.doi.org/10.1016/j.cnsns.2009.02.017.
9. Abdulkadhim MM, Mohsen AA, Al Husseiny HF, Hattaf K, Zeb A. Stability analysis and bifurcation for an bacterial meningitis spreading with stage structure: Mathematical modeling. *Iraqi J Sci.* 2024:2630–2648.
10. Khan H, Alzabut J, Gómez-Aguilar JF, Alkhazan A. Essential criteria for existence of solution of a modified-ABC fractional order smoking model. *Ain Shams Eng J.* 2024;15(5):102646.
11. Brhane KW, Ahmad AG, H. Hina, et al Mathematical modeling of cholera dynamics with intrinsic growth considering constant interventions. *Sci Rep.* 2024;14:4616. http://dx.doi.org/10.1038/s41598-024-55240-0.
12. Mukandavire Z, Tripathi A, C. Chiyaka, et al Modelling and analysis of the intrinsic dynamics of cholera. *Differ Equ Dyn Syst.* 2011;19:253–265. http://dx.doi.org/10.1007/s12591-011-0087-1.
13. Kennedy JO, Okaka A, Frankline T. A mathematical model on the dynamics of in-host infection cholera disease with vaccination. *Discrete Dyn Nat Soc.* 2023:11. http://dx.doi.org/10.1155/2023/1465228, 1465228, 2023.
14. Wang X, Wang J. Modeling the within-host dynamics of cholera: bacterial–viral interaction. *J Biol Dyn.* 2016;11(sup2):484–501. http://dx.doi.org/10.1080/17513758.2016.1269957.
15. AL-arydah M, Mwasa A, Tchuenche J, Smith R. Modeling cholera disease with education and chlorination. *J Biol Syst.* 2013;21:1–20.
16. Mohsen A, Hattaf K. Dynamics of a generalized fractional epidemic model of COVID-19 with carrier effect. *Adv Syst Sci Appl.* 2022;22(3):36–48. http://dx.doi.org/10.25728/assa.2022.22.3.1172.
17. Ilhem G, Kouche M, Ainseba B. Stability analysis of a fractional-order SEIR epidemic model with general incidence rate and time delay. *Math Methods Appl Sci.* 2023;46(9):10947–10969. http://dx.doi.org/10.1002/mma.9161.
18. Aqeel A, Muhammad F, Abdul G, Mustafa I, Ozair AM, Ndolane S. Analysis and simulation of fractional order smoking epidemic model. *Comput Math Methods Med.* 2022;2022:16. http://dx.doi.org/10.1155/2022/9683187, 9683187.
19. He Y, Wang Z. Stability analysis and optimal control of a fractional cholera epidemic model. *Fractal Fract.*. 2022;6(3):157. http://dx.doi.org/10.3390/fractalfract6030157.
20. Khatua A, Kar TK, Jana S. Global dynamics and optimal control of a nonlinear fractional-order cholera model. *Nonlinear Anal Model Control.* 2024;29(2):265–285. http://dx.doi.org/10.15388/namc.2024.29.34220.

21. Helikumi M, Lolika PO. A note on fractional-order model for cholera disease transmission with control strategies. *Commun Math Biol Neurosci*. 2022;2022:30.
22. Regassa CK, Purnachandra RK, Kenassa EG. Fractional derivative and optimal control analysis of cholera epidemic model. *J Math Univ Tokushima*. 2022;2022:17. 9075917.
23. Cui X, Xue D, Pan F. A fractional SVIR-B epidemic model for cholera with imperfect vaccination and saturated treatment. *Eur Phys J Plus*. 2022;137:1361. http://dx.doi.org/10.1140/epjp/s13360-022-03564-z.
24. Ahmed I, Akgül A, Jarad F, et al A Caputo–Fabrizio fractional-order cholera model and its sensitivity analysis. *Math Model Numer Simul Appl*. 2023;3(2):170–187. http://dx.doi.org/10.53391/mmnsa.1293162.
25. Khan H, Ahmed S, Alzabut J, Azar AT. A generalized coupled system of fractional differential equations with application to finite time sliding mode control for Leukemia therapy. *Chaos Solitons Fractals*. 2023;0174:113901.
26. Khan H, Alzabut J, Gulzar H. Existence of solutions for hybrid modified ABC-fractional differential equations with p-Laplacian operator and an application to a waterborne disease model. *Alexandria Eng J*. 2023;70:665–672.
27. Xu C, Liao M, Farman M, Shehzad A. Hydrogenolysis of glycerol by heterogeneous catalysis: A fractional order kinetic model with analysis. *MATCH – Commun Math Comput Chem*. 2023;91(3):635–664. http://dx.doi.org/10.46793/match.91-3.635X.
28. Xu C, Lin J, Zhao Y, et al New results on bifurcation for fractional-order octonion-valued neural networks involving delays. *Network*. 2024:1–53. http://dx.doi.org/10.1080/0954898X.2024.2332662, Epub ahead of print. PMID: 38578214.
29. Li P, Shi S, Xu C, et al Correction to: Bifurcations, chaotic behavior, sensitivity analysis and new optical solitons solutions of Sasa-Satsuma equation. *Nonlinear Dynam*. 2024;112:15521. http://dx.doi.org/10.1007/s11071-024-09792-5.
30. Muhseen AA, Zhou X. On the dynamical behaviors of a cholera model with holling type II functional response. *Al-Nahrain J Sci*. 2016;19(1):156–167.
31. Denu D, Kermausuor S. Analysis of a fractional-order COVID-19 epidemic model with lockdown. *Vaccines*. 2022;10(11):1773. http://dx.doi.org/10.3390/vaccines10111773.
32. Horn RA, Johnson CR. *Matrix analysis*. Cambridge University Press; 1985.
33. Arriola L, Hyman J. Forward and adjoint sensitivity analysis with applications in dynamical systems. In: *Lecture notes in linear algebra and optimization*. 2005.